GENG4412 Engineering Research Project Part 2

Final Report

REV Hydrofoil Board and Jet Ski Gen 2

Christopher A. Franz

23326375

School of Engineering, University of Western Australia

Supervisor: Thomas Bräunl

School of Engineering, University of Western Australia

Word count: 7917

School of Engineering

University of Western Australia

Submitted: 20 May 2026

Acknowledgements

I would like to sincerely thank Thomas Bräunl for his supervision, guidance, and support throughout this project.

I would also like to thank Tizzano Wehrli for his technical support, assistance, and guidance throughout the project, particularly regarding the active stabilisation system and foiling control architecture.

Finally, I would like to thank my family for their ongoing encouragement, patience, and support throughout the completion of this project and my degree.

Project Summary

The REV Hydrofoil Board and Hydrofoil Jet Ski Generation 2 project focused on the development of an actively stabilised electric hydrofoil system using low-cost embedded electronics, servo-actuated control surfaces, and additive manufacturing techniques. The project formed part of the University of Western Australia's Renewable Energy Vehicle (REV) laboratory research into sustainable electric marine transportation and advanced hydrofoil technologies.

The primary objective of the project was to design and validate an active foil control system capable of automatically stabilising an electric hydrofoil platform during operation. A donated foil board and mast assembly were modified to incorporate a custom-designed front hydrofoil wing featuring servo-driven ailerons, onboard sensors, and real-time stabilisation control. The hydrofoil board also acted as a rapid prototyping platform for technologies intended for integration into the larger Hydrofoil Jet Ski Generation 2 platform.

The electrical control system was built around a LilyGO ESP32-S3 microcontroller integrated with a BNO085 inertial measurement unit, waterproof ultrasonic sensor, and Micro Maestro servo controller. The system implemented closed-loop PID stabilisation algorithms to actively control foil position in response to measured roll, pitch, and ride height disturbances. Wireless web-based tuning and onboard telemetry monitoring were also incorporated to support testing and system development.

Mechanically, the custom hydrofoil wing was designed using Autodesk Fusion and manufactured using large-format FDM 3D printing with PETG filament. Structural reinforcement was achieved using embedded aluminium extrusion and stainless-steel pivot rods to support the actively controlled rear aileron surfaces. The NACA 2412 aerofoil profile was selected due to its stable lift characteristics and suitability for low-speed hydrofoil operation.

Testing demonstrated that the active stabilisation system successfully responded to roll and pitch disturbances during real-world hydrofoil operation. The servo-actuated control surfaces and onboard sensing systems were capable of maintaining partial stability while foiling. However, the larger 3D printed wing significantly increased hydrodynamic drag compared to the original factory hydrofoil, reducing the achievable operating speed from approximately 24 km/h to 12 km/h. This reduced lift generation and required manual rider input to assist the board onto foil during operation.

Several engineering challenges were encountered throughout development, including waterproofing failures, print instability during large-format manufacturing, dimensional inaccuracies in printed components, and structural failures within the wing mounting system. These issues highlighted the limitations of using large-scale FDM printed thermoplastic structures in high-load marine environments. Despite these challenges, the project successfully validated the concept of active hydrofoil stabilisation using low-cost embedded systems and rapid prototyping methods.

Overall, the project established a strong technical foundation for future development within the REV Hydrofoil Jet Ski Generation 2 platform. The work provided valuable insight into hydrofoil stabilisation control, waterproof marine electronics, structural reinforcement strategies, and hydrodynamic optimisation for electrically powered hydrofoil systems.

Introduction

As the global focus shifts away from fossil fuels and towards more sustainable energy solutions, electrically powered vehicles have rapidly emerged across multiple industries. The automotive sector has led this transition through the widespread adoption of electric vehicles (EVs), driven by advances in battery technology, increasing environmental awareness, and stricter emissions regulations. This movement has also begun extending into the maritime industry, where traditional fossil-fuel-powered propulsion systems are being reconsidered due to their significant contribution to greenhouse gas emissions and environmental degradation. In response to growing climate concerns, organisations such as the International Maritime Organization (IMO) have introduced ambitious emissions reduction targets, aiming to reduce shipping-related greenhouse gas emissions by at least 50% by 2050 compared to 2008 levels. [1] This has accelerated the development of cleaner and more energy-efficient marine transport technologies.

Figure 1 REV Electric Jet Ski [3]

The University of Western Australia's Renewable Energy Vehicle (REV) laboratory has played a significant role in the development of electric marine propulsion systems and hydrofoil-based watercraft over the past decade. Early work within the REV program focused on the development of Australia's first electric jet ski in 2013 [2], demonstrating the feasibility of replacing traditional internal combustion propulsion systems with battery-electric drivetrains for recreational marine applications [3]. This project highlighted both the environmental advantages and the engineering challenges associated with electric marine transport, particularly the limitations imposed by battery energy density and hydrodynamic drag.

Building on this foundation, the REV laboratory progressed into hydrofoil-assisted marine systems with the development of the Hydrofoil Electric Jet Ski (Generation 1) in 2019, known as the WaveFlyer project [4]. Developed in collaboration with Electro.Aero, the WaveFlyer utilised an actively stabilised hydrofoil propulsion system that allowed the craft to rise above the water surface during operation, significantly reducing drag and improving efficiency [5]. The hydrofoil configuration enabled the vehicle to achieve substantially greater energy efficiency compared to

conventional electric jet skis while also providing a quieter and zero-emission alternative for recreational marine transport [5].

Figure 2 REV Electric Hydrofoil Jet Ski (Generation 1) [5]

Following the success of the first-generation hydrofoil jet ski, further research within the REV laboratory expanded into smaller-scale hydrofoil platforms, including the Small Hydrofoil Boat project in 2024 and 2025. These projects continued to investigate active stabilisation systems, lightweight electrical architectures, and hydrodynamic optimisation for electrically powered marine vehicles [6], [7]. The research conducted through these platforms established a strong technical foundation for the development of increasingly advanced hydrofoil systems capable of improved efficiency, stability, and rider accessibility.

The current REV Hydrofoil Board and Hydrofoil Jet Ski Generation 2 project represents the next stage in this ongoing research progression. Unlike earlier platforms that primarily validated the concept of hydrofoil-assisted electric propulsion, the Generation 2 system focuses heavily on the development of an advanced active foil control backbone using low-cost embedded hardware. The project aims to improve stability, responsiveness, and scalability through the implementation of real-time control systems using ESP32 LilyGO microcontrollers, active servo-controlled foil surfaces, and future CAN bus integration for distributed control architectures.

Figure 3 REV Hydrofoil Boat 2024 [6]

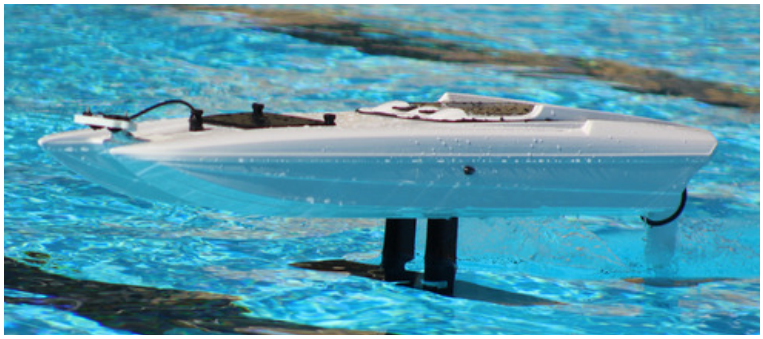

Figure 4 REV Hydrofoil Boat 2025 [7]

As part of this development pathway, the hydrofoil board is being used as an agile testing platform for active stability algorithms and embedded control validation. This smaller-scale platform enables rapid prototyping and flight testing of the control systems before they are transferred to the larger Hydrofoil Jet Ski Generation 2 platform. In parallel, the Generation 2 jet ski is being developed with upgraded electrical infrastructure, including a custom backbone PCB, integrated Battery Management System (BMS), and modular communication architecture designed specifically for the demanding marine environment.

Literature Review

Hydrofoil technology has become an increasingly important area of research within modern marine transportation due to its ability to significantly reduce hydrodynamic drag and improve vessel efficiency. Unlike conventional displacement or planning hulls, hydrofoils generate lift through submerged wing structures that raise the vessel above the water surface during operation, reducing wetted surface area and therefore lowering resistance forces. Although hydrofoil concepts date back to the late nineteenth century, significant advancements in foil design, materials, and hydrodynamic modelling have accelerated research into their application for both recreational and commercial marine vessels [8]. Modern studies have focused heavily on optimising hydrofoil geometry, including foil profile selection, aspect ratio, chord length, and incidence angle, in order to minimise propulsion power requirements while maintaining vessel stability and seakeeping performance [8]. These developments have become increasingly important as industries worldwide transition toward cleaner and more energy-efficient transport technologies.

The growing interest in electric marine propulsion has further increased the relevance of hydrofoil-assisted vessels due to the strict energy limitations imposed by battery-electric systems. Recent research conducted by Chalmers University of Technology and SSPA demonstrated that hydrofoil systems can reduce vessel resistance and fuel consumption by up to 80%, substantially improving the operational range of electric marine vehicles [9]. By lifting the hull clear of the water, hydrofoils dramatically decrease drag forces, enabling electric vessels to operate more efficiently at higher speeds while reducing overall energy consumption [9]. In addition to improving efficiency, electric hydrofoil vessels provide substantial environmental benefits through the elimination of tailpipe emissions, reduced underwater noise pollution, and decreased reliance on fossil fuels. Modern hydrofoil systems also benefit from advancements in lightweight carbon-fibre composite construction, allowing hydrofoils to operate efficiently under high loads while maintaining structural rigidity [9]. As a result, hydrofoil technology is increasingly viewed as a critical enabling technology for the future development of sustainable high-performance electric marine transportation systems.

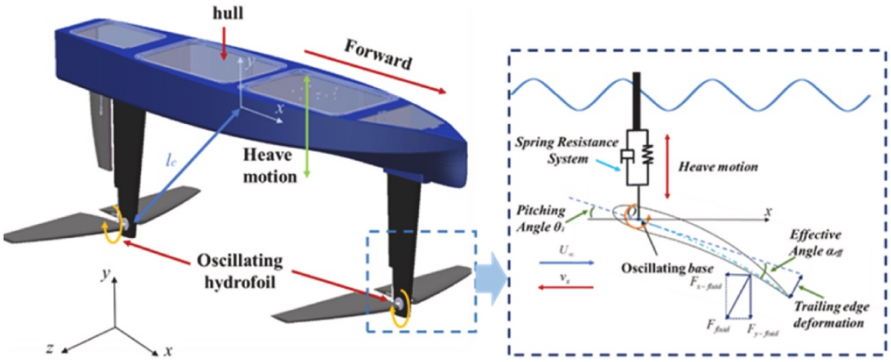

Figure 4 Hydrofoil Boat Free Body Diagrams [10]

Hydrofoil performance is also heavily influenced by the structural behaviour of the foil itself, particularly under varying wave and loading conditions. Traditional hydrofoil systems commonly utilise rigid foil geometries due to their structural simplicity and predictable hydrodynamic characteristics. However, recent research has demonstrated that flexible hydrofoils may provide improved propulsion efficiency and energy extraction capabilities in wave-powered marine systems [10]. Zhang et al. investigated the dynamic interaction between hydrofoil flexibility and propulsion performance using coupled fluid-structure interaction modelling to simulate real-world operating conditions [10]. Their research showed that the bending and pitching behaviour of hydrofoils significantly affects lift generation, thrust production, and overall vessel efficiency. The study further demonstrated that adaptive or flexible hydrofoil structures can better respond to changing wave conditions, allowing improved energy transfer and reduced hydrodynamic losses compared to

conventional rigid foil designs [10]. These findings highlight the importance of advanced hydrodynamic modelling and active foil optimisation in the development of efficient next-generation hydrofoil systems, particularly for electrically powered and wave-assisted marine vehicles.

Project Objectives

Hydrofoil Electric Jet Ski

The objective of this project is to develop a robust and modular electrical backbone for the REV Hydrofoil Jet Ski. This includes refining the previous electrical system and implementing staged testing capabilities for the ESP32 control modules through the use of jumper connections within the communication bus. Custom ESP32 modules will be developed to manage front and rear foil control, steering and throttle input, and motor control within a distributed architecture.

To support reliable system integration, Controller Area Network (CAN) bus communication will be implemented across all modules using a Maretron marine-grade connector backbone. This will provide reliable low-latency communication between subsystems while improving maintainability and scalability within the marine environment.

The project will also integrate and configure the Battery Management System (BMS), including wiring, commissioning, custom battery connection bars, and charging system integration. The BMS will provide battery monitoring, charging management, and fault detection to ensure safe and reliable operation. Additional objectives include contributing to the overall electrical architecture, component selection, and documentation required to support a scalable renewable-energy marine platform.

E-Foil Board

The first objective of this stage is to develop a functional electrically powered foil board platform, either by acquiring an existing e-foil board or modifying a conventional wind foiling board with an electric propulsion system. This provides a flexible and cost-effective platform for active foil development.

A major objective is the design and fabrication of a custom actively controlled front foil wing. The original wing will be replaced with a newly developed design modelled using CAD software and manufactured through large-scale 3D printing. The wing will incorporate pivot mechanisms and servo-driven actuation to enable active adjustment of foil geometry during operation.

Additional objectives include the development of a waterproof electronics enclosure, waterproofing of the servo systems, and design of the mechanical linkage mechanisms required for foil actuation. These systems will enable real-time adjustment of the foil surfaces to improve stability, manoeuvrability, and ride performance.

The final objective is the implementation of an automatic foil stabilisation system using a TTGO controller, onboard sensors, and real-time control algorithms. Unlike conventional e-foil systems that rely on rider-controlled foil adjustment, the developed platform will use continuous automatic foil control to maintain stability, compensate for disturbances, and improve overall handling and safety during operation.

Design Constraints

The design of the E-Foil Board was constrained by the requirement to integrate all newly developed systems with the existing donated board and mast assembly. Rather than designing a new platform, the active foil system had to adapt to the pre-existing geometry and mounting provisions, creating significant mechanical and dimensional limitations throughout development.

One of the main constraints involved mounting the custom front foil wing to the existing mast assembly. The wing and actuation system were required to use the original mounting hole pattern and interface dimensions, limiting mounting positions, fastener spacing, and wing geometry. As a result, the wing pivots, servo linkages, and support structures had to be designed around fixed connection points rather than being fully optimised. These limitations also influenced wing dimensions, pivot placement, and the internal reinforcement structure required to transfer hydrodynamic loads safely into the mast assembly.

The placement of the control electronics was also limited by the existing board structure. The waterproof enclosure used the pre-existing camera mounting location, avoiding major hull modifications while providing a secure mounting point. However, this restricted enclosure dimensions and component arrangement, including the TTGO controller, wiring, waterproof cable glands, and power distribution systems. The enclosure also needed to remain compact enough to avoid interfering with rider movement while maintaining waterproof sealing.

Additional electronic constraints were introduced by the ESP32 LilyGO T-S3 controller. Although it provided integrated wireless communication and sufficient processing capability, the controller offered limited available GPIO pins after accounting for onboard peripherals and communication interfaces. This restricted the number of sensors, actuators, and auxiliary devices that could be connected, requiring careful pin allocation between servo outputs, sensor inputs, and communication peripherals.

Manufacturing constraints also resulted from the use of large-format FDM 3D printing for the wing and mechanical components. While FDM printing enabled rapid prototyping and low-cost fabrication, the printed parts had lower structural strength and impact resistance than composite or machined alternatives. The layer-by-layer process also introduced anisotropic mechanical properties, requiring careful consideration of print orientation, load paths, and reinforcement strategies. Printed components were additionally susceptible to layer delamination, creep under sustained loading, and thermal limitations depending on the filament material.

The marine environment further constrained material selection, as prolonged water exposure and ultraviolet radiation can degrade common thermoplastics over time. As a result, the wing structure and mounting systems required increased wall thicknesses, internal reinforcement, and conservative loading assumptions to ensure reliable operation during testing.

Finally, the integration of waterproof servos and moving foil mechanisms introduced additional reliability constraints. Limited mounting space within the wing restricted servo sizing and linkage geometry, requiring compromises between available torque, mechanical leverage, response speed, and structural rigidity.

Design Process

Electrical Design E-Foil Board

Microcontroller

The LilyGO ESP32-S3 was selected as the primary controller for the active foil control system due to its balance of functionality, affordability, and ease of integration. A major advantage of the controller was its integrated display, which enabled real-time monitoring and debugging without requiring an external screen. This reduced system complexity, wiring requirements, and enclosure space while simplifying testing and development. The controller was also relatively inexpensive, making it suitable for the constrained project budget while still providing sufficient performance for active foil control applications.

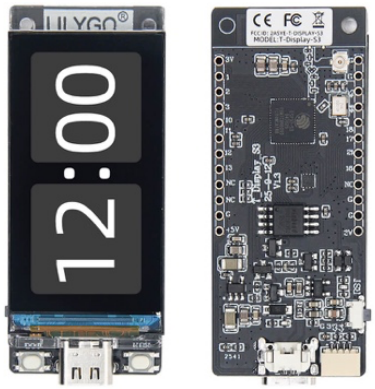

Figure 5 LilyGo T-Display S3 [11]

Another key factor in the selection process was the availability of multiple GPIO pins and the dual-core processing architecture of the ESP32-S3. The GPIO interfaces enabled integration with servo motors, sensors, power monitoring systems, and communication peripherals within a compact platform. The dual-core processor allowed control tasks, sensor acquisition, and display updates to operate concurrently, improving overall system responsiveness and stability during operation [11]. Although GPIO availability later became a design limitation, the controller still provided adequate flexibility for the required implementation.

The ESP32-S3 was also selected due to its familiarity and widespread use throughout previous engineering projects completed during the degree. Prior experience with the ESP32 ecosystem, programming environment, and debugging tools reduced development time and simplified software implementation. In addition, the controller benefits from extensive online documentation and strong community support, providing accessible resources for troubleshooting and ongoing development throughout the project.

Servo Motor

The HF3240SMG Waterproof Servo was selected for the active foil actuation system due to its high torque output, compact form factor, and IP68 waterproof rating, making it suitable for marine operation [12]. The servo provided sufficient torque capacity for the calculated hydrodynamic loading conditions while remaining compact enough to integrate within the limited internal space of the wing structure. It also offered a cost-effective solution compared to industrial-grade waterproof actuators while still meeting the operational requirements of the project. Calculations validating the servo selection and torque requirements are presented in a later section of this thesis.

Figure 6 Hobby Fans Servo [12]

Although the servo was supplied with an IP68 waterproof rating, additional waterproofing measures were implemented to improve long-term reliability during continuous marine exposure. This involved disassembling the servo housing and applying silicone grease to the internal electrical components and printed circuit boards to provide an additional moisture barrier. Following

reassembly, the enclosure was resealed using black marine-grade silicone sealant to further reduce the likelihood of water ingress around housing joints and cable entry points.

These modifications were implemented to minimise the risk of corrosion, electrical failure, and moisture-related degradation during operation in harsh marine environments.

Servo Controller

The Micro Maestro 6-Channel USB Servo Controller was selected to manage servo actuation within the active foil control system due to its ability to generate stable and precise servo control signals independently from the ESP32-S3 controller. Offloading servo signal generation reduced processing overhead on the primary controller and improved overall reliability while handling tasks such as sensor acquisition, control calculations, and display updates [13].

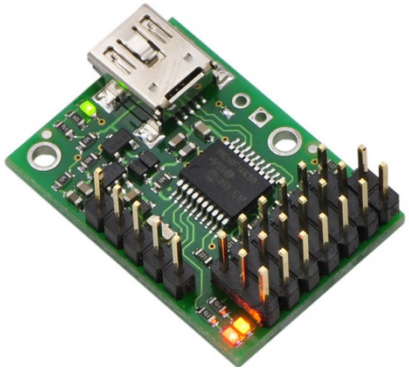

Figure 7 Micro Maestro Servo Controller [13]

A major advantage of the Micro Maestro controller was its ability to implement configurable position and movement limits for each servo output. This was important for protecting the mechanical foil system from overextension caused by incorrect sensor readings, software faults, or unexpected control outputs. By restricting servo travel range within the controller itself, the system provided an additional hardware-level safety layer to prevent damage to the wing structure, servo linkages, and pivot mechanisms.

The controller was also selected because it eliminated servo signal ghosting and unintended movement commonly observed during ESP32-S3 boot-up sequences. When servos are controlled directly from the ESP32, some GPIO pins can briefly output unstable states during startup, causing unwanted servo motion. The Micro Maestro isolated the servo system from these boot-time behaviours by independently managing PWM generation, ensuring stable servo positioning during power-up and reducing the risk of accidental foil movement or mechanical damage.

In addition, the controller supported multiple servo outputs within a compact form factor while providing simple USB and serial communication interfaces for integration, configuration, and debugging throughout development

Ultrasonic Sensor

The A02YYUW Waterproof Ultrasonic Sensor was selected to provide distance and height measurement capabilities for the active foil control system. The sensor was chosen due to its waterproof construction, compact size, and ability to provide non-contact distance measurements suitable for marine environments. It was intended to measure the relative height of the board above the water surface, allowing the control system to make automatic foil adjustments to improve stability during operation.

Figure 8 Waterproof Ultrasonic Sensor [14]

A major advantage of the A02YYUW sensor was its simple UART communication interface, which enabled straightforward integration with the ESP32-S3 controller while minimising GPIO usage [14]. This was important due to the limited number of available GPIO pins on the controller. The sensor also operated from a low-voltage power supply and provided adequate measurement range and response speed for the intended application. Its waterproof design made it

suitable for continuous exposure to water spray and wet operating conditions encountered during e-foil operation.

Compared to more advanced sensing technologies such as LiDAR or radar systems, the ultrasonic sensor provided a significantly lower-cost solution while still offering sufficient functionality for prototype-level active foil control and stability testing.

Battery and Voltage Regulation

A 2-cell (2S) 7.4 V 2000 mAh lithium polymer (LiPo) [15] battery was selected to power the active foil control system due to its compact size, lightweight construction, and ability to supply sufficient current for the project electronics. The battery powered the ESP32-S3 controller, Micro Maestro servo controller, ultrasonic sensor, and waterproof servos while maintaining a compact footprint suitable for integration within the waterproof enclosure. Its low mass also minimised additional weight on the foil board, reducing the impact on ride performance and stability.

Figure 9 Angry Snail Battery [15]

Figure 10 Buck Converter [16]

To provide stable operating voltages, a DC-DC buck converter rated for 6–30V input with a regulated 5 V output at up to 3A [16] was integrated into the power system. The converter stepped the 7.4V battery voltage down to a stable 5V supply for the ESP32-S3 controller and auxiliary electronics. This improved power stability and reduced the risk of voltage fluctuations affecting system performance during high servo loading conditions. The converter also provided a compact and low-cost solution suitable for the limited enclosure space.

The dedicated voltage regulator further improved reliability by electrically isolating sensitive control electronics from transient voltage drops and electrical noise generated by the servo motors during rapid actuation. This was particularly important for maintaining stable controller operation, accurate sensor readings, and reliable real-time foil adjustment within the active stabilisation system.

Inertial Measurement Unit

The Adafruit 9-DOF Orientation IMU Fusion Breakout - BNO085 was selected as the primary inertial measurement unit (IMU) for the active foil control system due to its integrated sensor fusion capabilities, compact form factor, and ability to provide stable real-time orientation data for closed-loop stabilisation control. The BNO085 combines accelerometer, gyroscope, and magnetometer data internally to output filtered orientation measurements, reducing the computational burden on the ESP32-S3 controller.

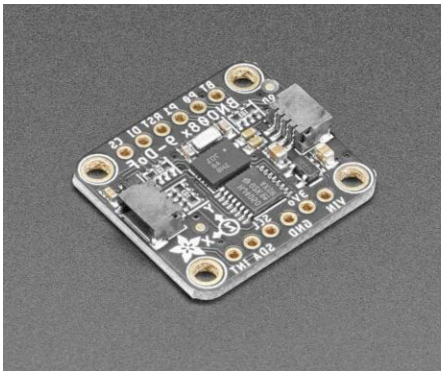

Figure 11 Adafruit BNO085 IMU [20]

A major advantage of the BNO085 was its onboard sensor fusion processor, which outputs quaternion and rotation vector data directly rather than requiring complex filtering algorithms to be implemented on the microcontroller. This simplified software development and improved orientation accuracy and stability during dynamic operation. The sensor was used to measure roll, pitch, and yaw orientation of the foil board, allowing the control system to continuously adjust the active foil surfaces to maintain stability during operation.

The BNO085 was also selected for its relatively high update rate and good motion tracking performance, both important for active stabilisation systems operating in rapidly changing environments. The sensor supported I2C communication, enabling straightforward integration with the ESP32-S3 while minimising wiring complexity. In addition, the widespread use of the BNO085 within robotics, drone, and balancing applications meant extensive documentation, libraries, and development resources were readily available, simplifying integration and troubleshooting throughout the project.

Electrical Wiring

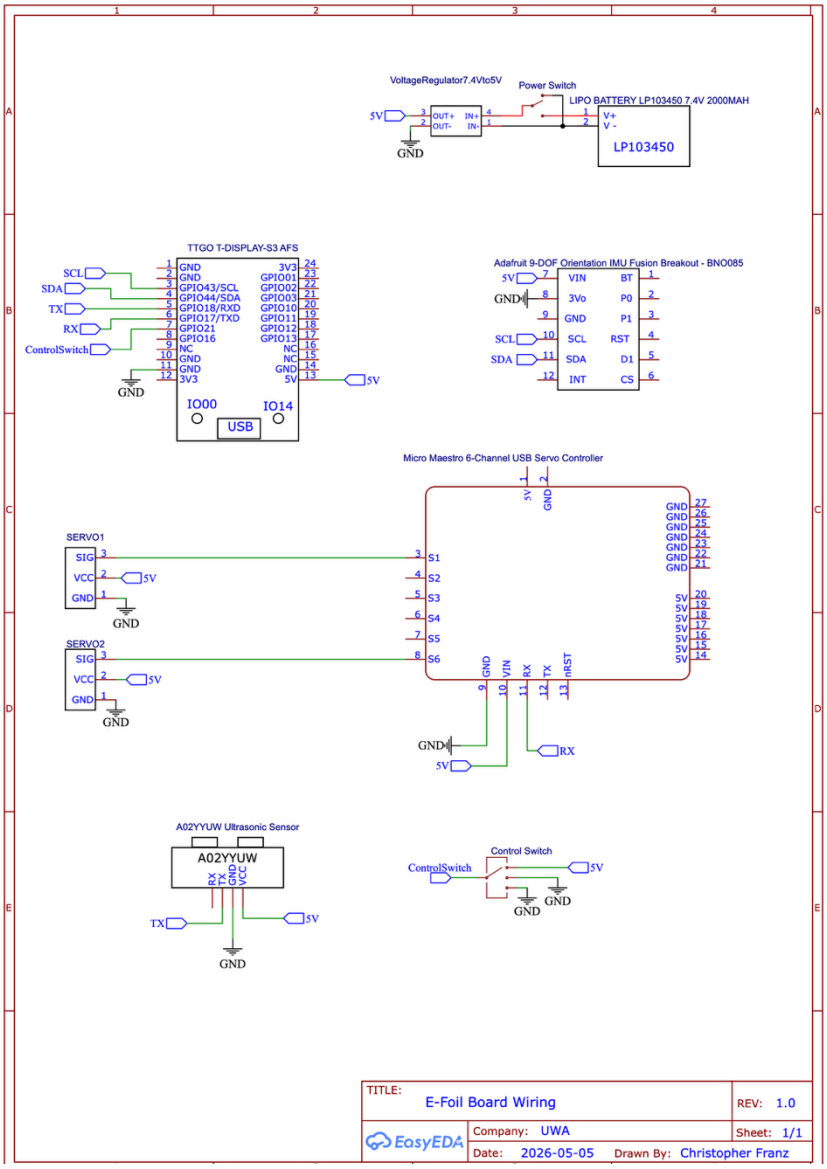

Figure 12 Wiring Diagram For E-Foil Board

Mechanical Design Process

Wing Material

PETG (Polyethylene Terephthalate Glycol) filament was selected as the primary material for the FDM-printed structural components of the active foil system due to its combination of strength, durability, and moisture resistance. Compared to PLA, PETG provides improved impact resistance, higher temperature tolerance, and greater flexibility, making it more suitable for mechanically loaded marine applications. These properties were important for the active foil wing and mounting structures, which experience continuous hydrodynamic loading, vibration, and impact forces during operation. PETG also demonstrated strong layer adhesion during printing, reducing the likelihood of delamination in highly stressed components.

Figure 13 PETG Roll [21]

Although stronger materials such as carbon fibre composites or marine-grade wood could provide improved structural stiffness and performance, they were not selected due to increased manufacturing complexity, tooling requirements, and fabrication time. In comparison, PETG allowed components to be rapidly manufactured, modified, and reprinted using the available large-format FDM printing equipment. This significantly simplified the iterative design process and enabled rapid prototyping of different foil geometries and mechanical configurations while remaining within the project's time and budget constraints.

Structural Support Material

A 19 mm aluminium extrusion was selected for the internal structural support of the active foil wing due to its high strength-to-weight ratio, corrosion resistance, and ease of integration within the printed wing structure. The extrusion provided significantly greater rigidity and load-bearing capability than printed plastic components alone, allowing hydrodynamic forces to be distributed more effectively throughout the structure. To maximise strength, the extrusion was embedded directly within the wing during assembly, enabling it to function as the primary load-bearing member while reducing bending and flexing under hydrodynamic loading. This also improved structural integration while maintaining the external aerodynamic profile of the foil.

Figure 14 Aluminium Extrusion [22]

A 6 mm stainless steel rod was selected as the pivot shaft for the actively controlled aileron section due to its high strength, wear resistance, and corrosion resistance in marine environments. Similar to the aluminium reinforcement, the pivot rod was embedded within the wing structure to improve strength and alignment of the moving foil section. Embedding the shaft allowed rotational loads generated by the servo-driven actuation system to be transferred more effectively through the wing while reducing localised stress concentrations around the pivot points.

Figure 15 6mm Stainless Steel Rod [23]

The combination of embedded aluminium extrusion and stainless-steel reinforcement significantly improved rigidity and durability while still using lightweight FDM-printed PETG components for the aerodynamic surfaces. This hybrid construction approach balanced structural performance with manufacturing simplicity and allowed the active foil system to be fabricated using available workshop resources and additive manufacturing equipment.

Wing Profile

The wing profile selected for the active hydrofoil system was the NACA 2412 aerofoil profile. The NACA 2412 profile was chosen due to its well-documented aerodynamic characteristics, moderate camber, and stable lift behaviour across a range of operating conditions. The aerofoil consists of a maximum camber of 2% located at 40% of the chord length, with a maximum thickness of 12% of the chord. [17] These characteristics provide a balance between lift generation, structural thickness, and predictable flow behaviour, making the profile suitable for low-speed hydrofoil and control surface applications.

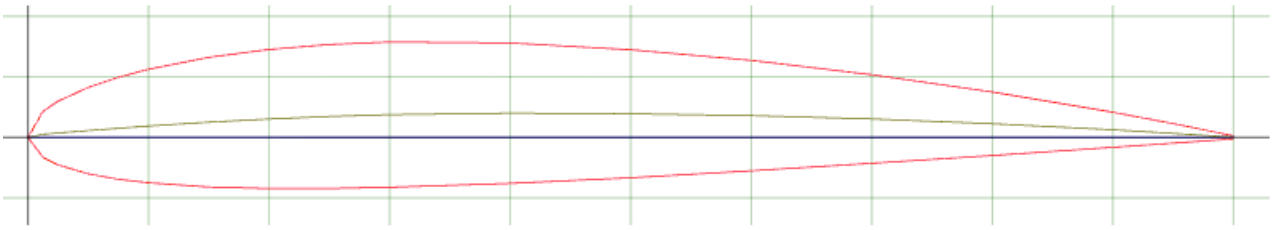

Figure 16 NACA 2414 Profile [15]

A major reason for selecting the NACA 2412 profile was its ability to generate relatively high lift at low to moderate Reynolds numbers while maintaining stable and predictable aerodynamic performance. Research into the aerodynamic characteristics of the NACA 2412 profile has shown that it possesses favourable lift-to-drag properties and smooth aerodynamic behaviour over varying angles of attack [18]. This behaviour was considered beneficial for the active foil system, where stable and controllable lift generation is important for maintaining ride stability and responsive foil adjustment. Compared to symmetrical aerofoils such as the NACA 0012, the cambered NACA 2412 profile naturally produces greater lift at the same angle of attack due to its asymmetrical geometry.

The 12% thickness of the profile was also advantageous from a structural perspective, as it provided sufficient internal volume to accommodate the embedded aluminium reinforcement, stainless steel pivot rod, servo mounting systems, and mechanical linkage components within the wing body. In addition, the relatively thick profile improved manufacturability using FDM 3D printing by allowing stronger internal wall sections and reinforcement structures to be incorporated without excessively reducing the aerodynamic performance of the wing. Previous applications of the NACA 2412 profile in aircraft and aerodynamic research also demonstrated its stable handling characteristics and tolerance to minor surface imperfections, which was considered beneficial given the layer-based surface finish produced through [19].

Wing Design

The active foil wing was designed using CAD software within Autodesk Fusion to model the structural, mechanical, and aerodynamic features required for the project. An internal cavity was incorporated into the wing profile to house a 19 mm × 19 mm aluminium extrusion used for structural reinforcement. Material was removed from the forward section of the profile so the extrusion could be embedded while maintaining the external aerodynamic geometry. Embedding the extrusion improved rigidity and allowed hydrodynamic loads to be distributed more effectively throughout the assembly.

The actively controlled aileron section occupied approximately 33% of the overall wing chord length. This relatively large control surface was selected to maximise lift variation and control authority from small angular movements, compensating for the limited rotational travel available from the waterproof servo motor mounted within the wing structure. Each side of the wing was designed with a span of 440 mm, giving an overall wingspan of approximately 880 mm. This was based on the geometry of the original fixed foil supplied with the donated board, which had an approximate width of 820 mm. While the original foil featured a curved profile with a variable chord length reaching approximately 270 mm, the custom wing used a straight geometry with a constant chord width of 220 mm. This approximated the original lifting surface area while simplifying manufacturing and integration of the active aileron mechanism.

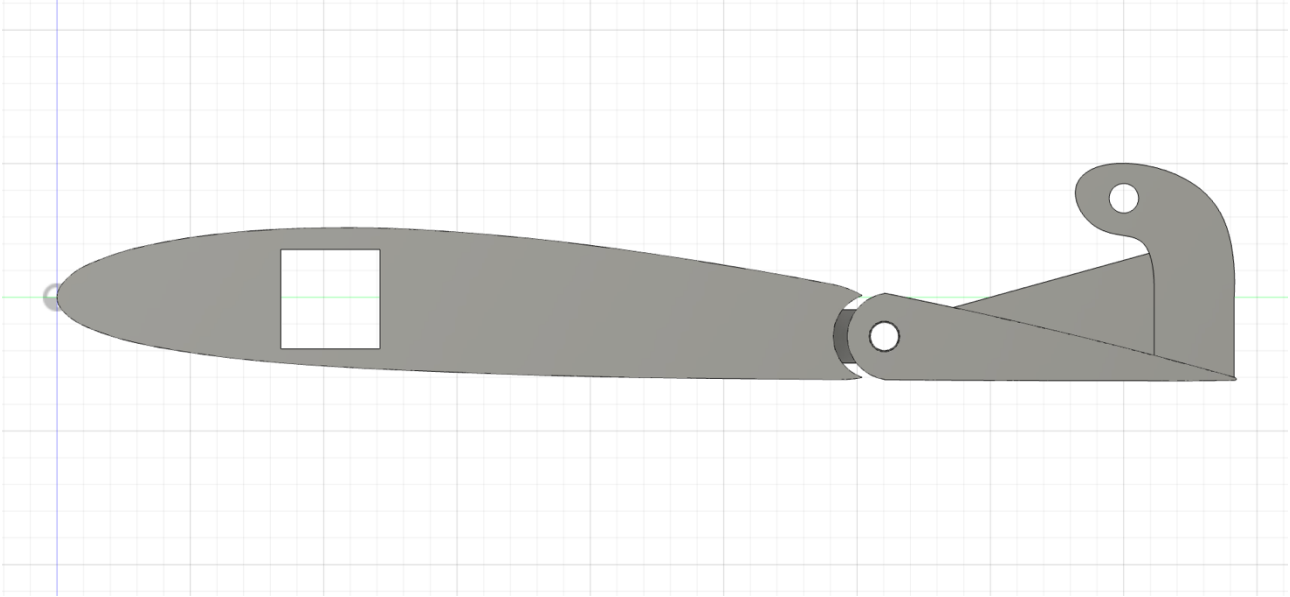

Figure 17 CAD Drawing of Wing Side Profile

A 6 mm diameter hole was extruded through the wing structure along the aileron pivot point to allow insertion of a 6 mm stainless steel pivot rod. This created a continuous structural pivot axis across the wing assembly, enabling smooth rotational movement of the actively controlled aileron while improving alignment and mechanical strength. Extending the pivot rod through the full width of the wing distributed rotational loads more evenly and reduced stress concentrations around mounting points.

The mounting interface was designed using a modular assembly approach, where components slid directly onto the embedded aluminium extrusion. This simplified alignment and assembly during manufacturing and testing while also improving maintainability and future design modification. The extrusion acted as the primary structural connection between wing sections, reducing reliance on

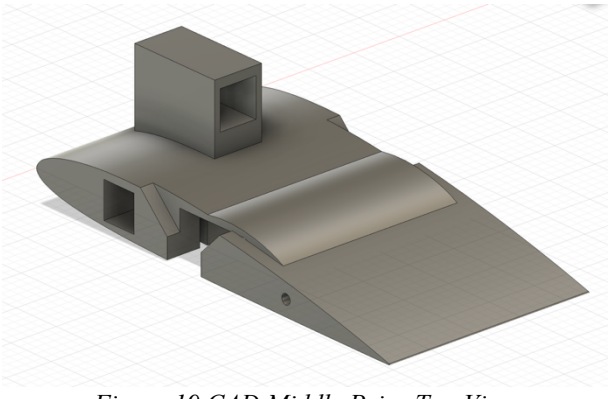

Figure 19 CAD Middle Peice Top View

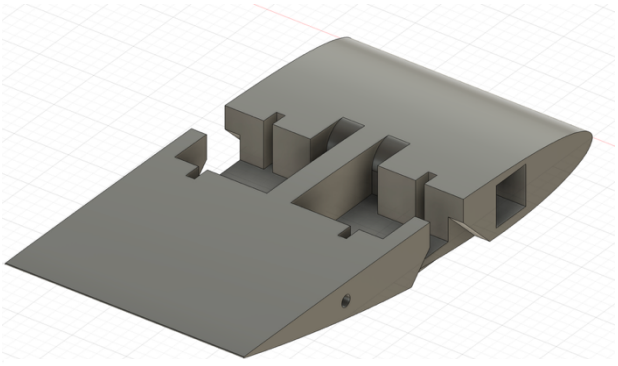

Figure 18 CAD Middle Piece Bottom View

adhesive bonding between printed PETG components and transferring loads through the internal metal reinforcement instead.

A central mounting section was designed to connect the wing assembly to the existing foil mast interface while also housing the waterproof servo motors used for aileron actuation. Integrating the servos into the centre section reduced external mounting complexity and maintained a compact structural layout. The mounting geometry aligned with the existing mast interface, allowing the active foil system to connect to the donated board hardware without major modification.

The waterproof servos were embedded into the underside of the centre profile, so the lower surface of the servo housings remained approximately flush with the lower aerodynamic surface of the wing. This minimised disturbance to hydrodynamic flow beneath the foil, where higher fluid velocities make the surface more sensitive to discontinuities. Due to wing thickness limitations and servo dimensions, the upper portion of the housings protruded above the wing surface. To address this, an aerodynamic fairing was incorporated into the upper profile to protect the exposed servos while reducing drag and turbulence.

Cut-outs were incorporated into the upper wing structure to provide clearance for servo horn movement. The servo horns protruded vertically through the wing surface and aligned with the rear aileron pivot geometry to simplify the linkage arrangement and improve force transfer efficiency. A hook-like protrusion was integrated into the moving control surface to provide a mounting point for the linkage rod connecting the servo horn to the rear aileron. A rigid linkage bar translated servo rotation directly into controlled aileron deflection, enabling active foil adjustment through a lightweight and mechanically simple control system.

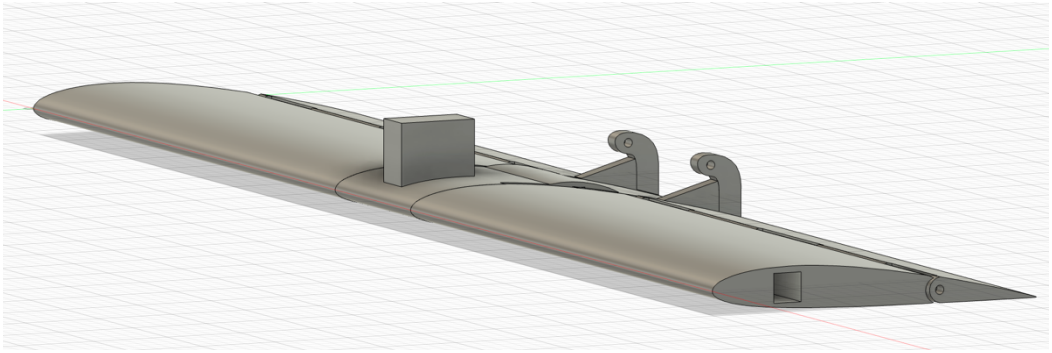

Figure 20 Final CAD Design of Wing

Final Build

Build Process

The manufacturing and assembly process of the active hydrofoil system involved the integration of large-scale 3D printed components, structural reinforcement members, active control surfaces, and waterproofed electronic systems. The primary hydrofoil wing sections were manufactured using large-format FDM 3D printing, allowing the major structural components to be produced as single sections rather than multiple segmented parts. This improved structural continuity and reduced the number of mechanical joints required throughout the wing assembly. Following printing, the components underwent post-processing to remove support material and prepare critical mounting surfaces and internal features for assembly.

Following fabrication, the main wing assembly was constructed around a 19 mm × 19 mm aluminium extrusion which acted as the primary internal structural member for the hydrofoil system. The printed wing sections were carefully fitted onto the aluminium extrusion and aligned to ensure correct positioning and rigidity throughout the wing structure. Once the primary wing sections were assembled, the active aileron control surfaces were integrated into the rear section of the wing.

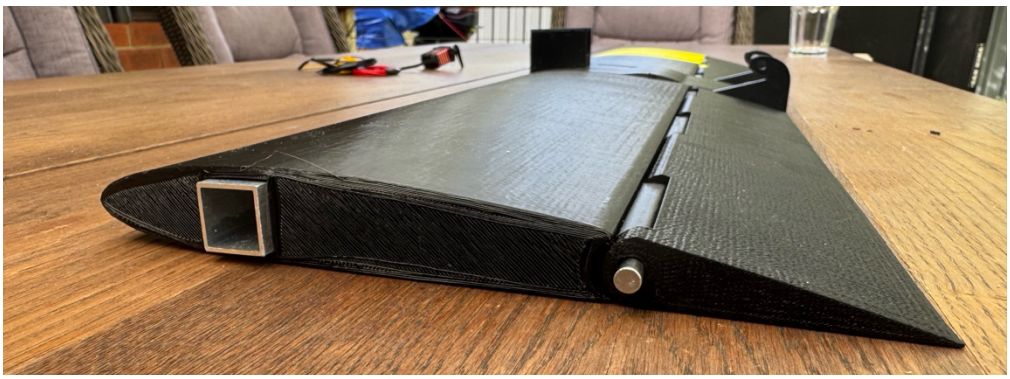

Figure 21 Final Wing Profile

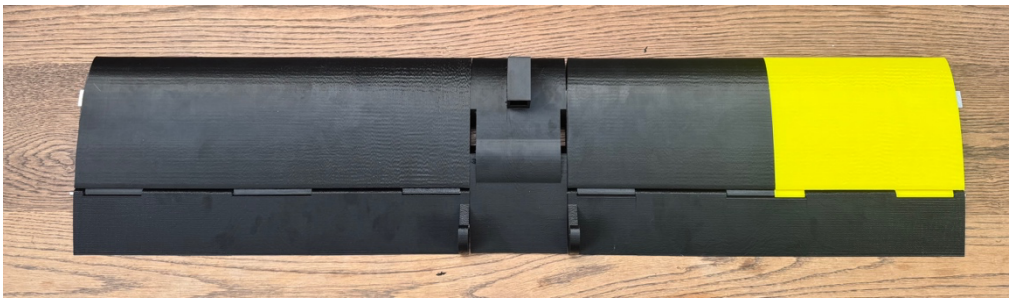

Figure 22 Final Wingspan

Each aileron was aligned with the mounting holes incorporated into the main wing structure and connected using a continuous 6 mm stainless steel pivot rod. The rod was inserted through the aileron hinge sections and corresponding wing supports to create the rotational axis required for active pitch control. Waterproof servos were then installed into dedicated servo housings integrated within the wing structure. A mechanical linkage was attached between the servo horn and the aileron control surface to translate servo rotation into controlled aileron movement. Careful alignment was required during this stage to ensure smooth rotational movement throughout the linkage system. The servos were secured within the housings using a combination of press-fit mounting and hot glue to prevent movement during operation and improve vibration resistance.

Figure 24 Aileron-Servo Horn Connection Rod

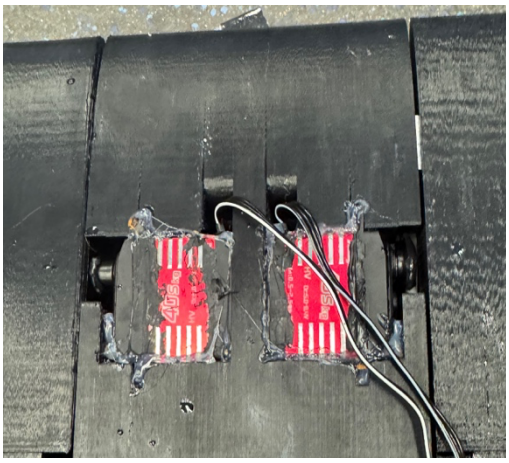

Figure 23 Servos Embedded in Housing'

Once the mechanical assembly was completed, the servo movement limits were configured and programmed using the Maestro servo controller. The control limits were adjusted to ensure the ailerons operated within the required angular range for active pitch control. Following programming, the complete wing structure was inspected and mechanically tested to verify correct operation of the active control surfaces.

Following mechanical assembly, the electronic systems were integrated and wired. All major electrical components, including the control electronics, power distribution systems, ultrasonic sensor, and waterproof servo connections, were mounted within waterproof enclosures to protect sensitive components during marine operation. A secondary waterproof enclosure was incorporated to house the system switches separately from the primary electronics compartment. Waterproof cable glands were installed on this secondary enclosure to allow electrical wiring to pass through the enclosure walls while maintaining environmental sealing around the cable entry points. To provide protected cable routing between the two enclosures, a custom joining pipe was designed and 3D printed. This joining structure allowed wiring to pass safely between the enclosures while improving cable management and assisting with the waterproof integrity of the electrical system.

Additional assembly work was completed for servo integration due to the standard servo cable lengths being insufficient for the final system layout. The servo wiring was extended to reach the main control electronics enclosure mounted on the board. Waterproof solder seal connectors were used to join the wire extensions, with the joined sections further protected using waterproof heat shrink tubing to provide insulation, strain relief, and moisture protection.

Figure 25 Final Electronics Box Internals

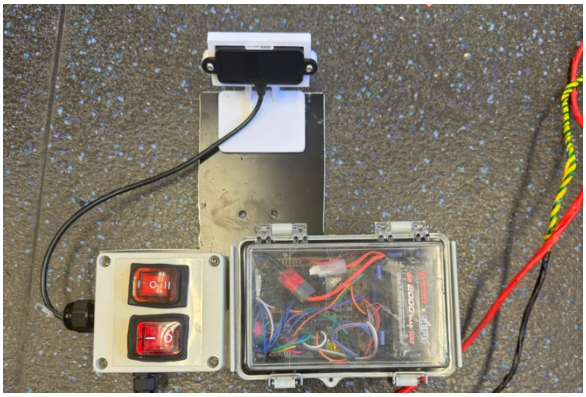

Figure 26 Electronics Boxes Mounted To Plate

To mount the electronic systems onto the board, a 3 mm aluminium composite sheet was cut and fabricated to act as a dedicated electronics mounting plate. The waterproof electronics enclosures, ultrasonic sensor, and associated hardware were mounted directly onto this plate, allowing the electrical system to be consolidated into a single removable assembly while improving cable organisation and accessibility. The completed mounting plate was then attached directly to the factory camera mounting points located on the board. Utilising the existing factory mounting structure simplified installation and avoided the need for permanent modifications to the board itself. Once mounted, all remaining electrical connections between the servos, sensors, switches, and control electronics were completed and tested to verify reliable system operation. Finally all components where mounted to the board.

Figure 27 Wing Mounted To E-Foil Board

Figure 28 Electrical Assembly Mounted To Board

Bill of Materials

Table 1 Bill of Materials for Custom Wing and Electronics

Item	Quantity	Price Per Unit ($)	Total Price ($)
LilyGo ESP32-S3	1	23.00	23.00
HF3240SMG Servo Motor	2	38.79	77.58
Micro Maestro Servo Controller	1	45.80	45.80
Ultrasonic DF Robot A02YYUW	1	36.20	36.20
7.4V 2000mAh 2S Battery	1	25.59	25.59
DC 30V to 5V Buck Converter	1	0.50	0.50
Adafruit 9-DOF Orientation IMU Fusion	1	46.45	46.45
AcbbMNS IP67 Waterproof Junction Box	1	29.99	29.99
IP65 Sealed ABS Flange Mount Enclosure	1	16.25	16.25
DPST 16A IP65 Weatherproof Rocker Switch	2	8.00	16.00
19x19x1.2 Aluminium Tube	1	13.04	13.04
6mm Stainless Steel Rod	1	27.95	27.95
DETA 16mm Black Cable Gland - 16mm	3	1.56	4.68
PETG 1KG Roll	2	17.99	35.98
		Total	$399.01

Software Build

The software architecture for the active hydrofoil control system was based on an existing framework originally developed for the REV hydrofoil boat project. Reusing this software significantly reduced development time while providing a proven foundation for implementing active foil stabilisation on the e-foil platform. The software was modified to suit the different mechanical geometry, sensor arrangement, and operating requirements of the foil board system, with additional functionality added for real-time tuning, user interaction, and operational mode switching. The primary control philosophy was based on automatic closed-loop stabilisation using multiple proportional-integral-derivative (PID) control loops. Rather than manually controlling foil position, the system continuously adjusted the foil surfaces in response to sensor feedback. This improved rider stability and reduced the amount of manual correction required during operation. Feedback from both the onboard inertial measurement unit (IMU) and ultrasonic height sensor was used to maintain stable foil behaviour in real time.

The first stage of the system involved the IMU, which provided roll, pitch, and yaw orientation data using quaternion-based motion estimation. This data was converted into Euler angles for use within the control loops. Separate PID controllers were implemented for roll and pitch stabilisation, allowing the system to independently correct unwanted rotational movement. Roll corrections balanced the left and right foil outputs, while pitch corrections controlled the rear ailerons to maintain stable longitudinal behaviour. An ultrasonic sensor was also incorporated to provide height-above-water measurements for altitude stabilisation. The altitude PID controller compared the measured ride height against a predefined cruising height setpoint, with the output dynamically adjusting the pitch angle setpoint. This created a cascaded control structure where the altitude controller generated the desired pitch target while the pitch controller adjusted the foil surfaces to achieve it. This layered approach improved responsiveness and allowed the board to compensate for rider movement and changing water conditions.

Servo outputs were generated through an external Micro Maestro servo controller rather than directly from the ESP32-S3. This improved signal stability and reduced servo jitter and boot-time ghosting behaviour. Final servo positions were calculated by combining roll and pitch PID outputs, allowing coordinated movement of the left and right control surfaces. By independently increasing or decreasing outputs on each side, the system could simultaneously stabilise roll and pitch motion. To improve usability during testing and tuning, a web server interface was integrated into the ESP32-S3 software, with the complete implementation provided in Appendix 1. The web server allowed wireless access to control settings and PID tuning parameters through a web browser without requiring a direct computer connection. This enabled rapid adjustment of control gains and operating parameters during live testing sessions. The integrated display on the LilyGO ESP32-S3 also provided live telemetry data including IMU readings, ride height measurements, memory usage, and overall system status information. A physical mode-switching system was additionally implemented, allowing the rider to transition the board into active foil mode during operation and alternate between settings/debug mode and fully automatic stabilisation mode depending on operational requirements.

Other Works (Jet Ski)

Contributions to the REV Hydrofoil Jet Ski project primarily focused on the development, integration, and implementation of the electrical systems architecture for the vehicle. A major component of this work involved the creation and organisation of detailed parts lists and system costings to support procurement, budgeting, and overall project planning. This included researching suitable electrical components, assisting with component selection decisions, and evaluating hardware based on factors such as performance, compatibility, environmental suitability, and cost constraints.

Significant involvement was also undertaken in the development and assembly of the battery and power distribution systems. This included wiring and integrating the Battery Management System (BMS) into the vehicle's electrical backbone to enable safe battery monitoring and operation. In addition, custom battery connection bars were designed and manufactured to provide secure high-current electrical connections between battery cells and associated power systems. Work was also completed to ensure compatibility between the battery system and the electric vehicle charging infrastructure used within the project, allowing the charging system to interface correctly with the battery pack and protection systems.

Further contributions were made toward the overall electrical design and integration of the hydrofoil jet ski platform. This included assisting with the design of the modular electrical architecture, contributing to communication system planning, and supporting the implementation of the distributed control systems used throughout the vehicle. Input was also provided into electrical layout considerations, wiring integration, and system-level design decisions to support the development of a scalable and maintainable marine electrical platform.

Results and Discussion

Results and Analysis

The completed active hydrofoil system was successfully manufactured, assembled, and tested within a real-world marine environment. Testing demonstrated the successful integration of large-scale FDM 3D printed hydrofoil structures, waterproof electronics, servo-actuated control surfaces, and closed-loop active stabilisation control. Throughout testing, the onboard sensors, waterproof servo systems, and control electronics operated reliably, with the active stabilisation system continuously responding to measured roll and pitch disturbances during operation. The testing process demonstrated that the concept of an actively controlled hydrofoil using embedded waterproof servos and low-cost control electronics was achievable within a prototype-level marine platform.

The primary limitation encountered during testing was the significantly increased hydrodynamic drag generated by the redesigned front hydrofoil wing. Compared to the original factory hydrofoil wing supplied with the donated board, the custom-designed wing featured a thicker aerodynamic profile, embedded structural reinforcement, integrated waterproof servos, and additional moving mechanical systems. While these modifications improved structural rigidity and enabled implementation of the active foil system, they also resulted in a considerable increase in hydrodynamic drag and overall system mass. This increased resistance placed a significantly larger load on the electric propulsion system and reduced the achievable operating speed of the board. Testing demonstrated that the original factory hydrofoil configuration was capable of speeds approaching 24 km/h, whereas the modified active hydrofoil system achieved a maximum speed of approximately 12 km/h. Due to this reduced speed, the board frequently struggled to naturally generate sufficient lift to rise onto foil during acceleration, requiring the rider to manually pump the board during take-off to assist foil transition. Once sufficient lift had been generated and the board successfully transitioned onto foil, stable hydrofoil operation could be achieved, although at a noticeably lower speed than the original configuration.

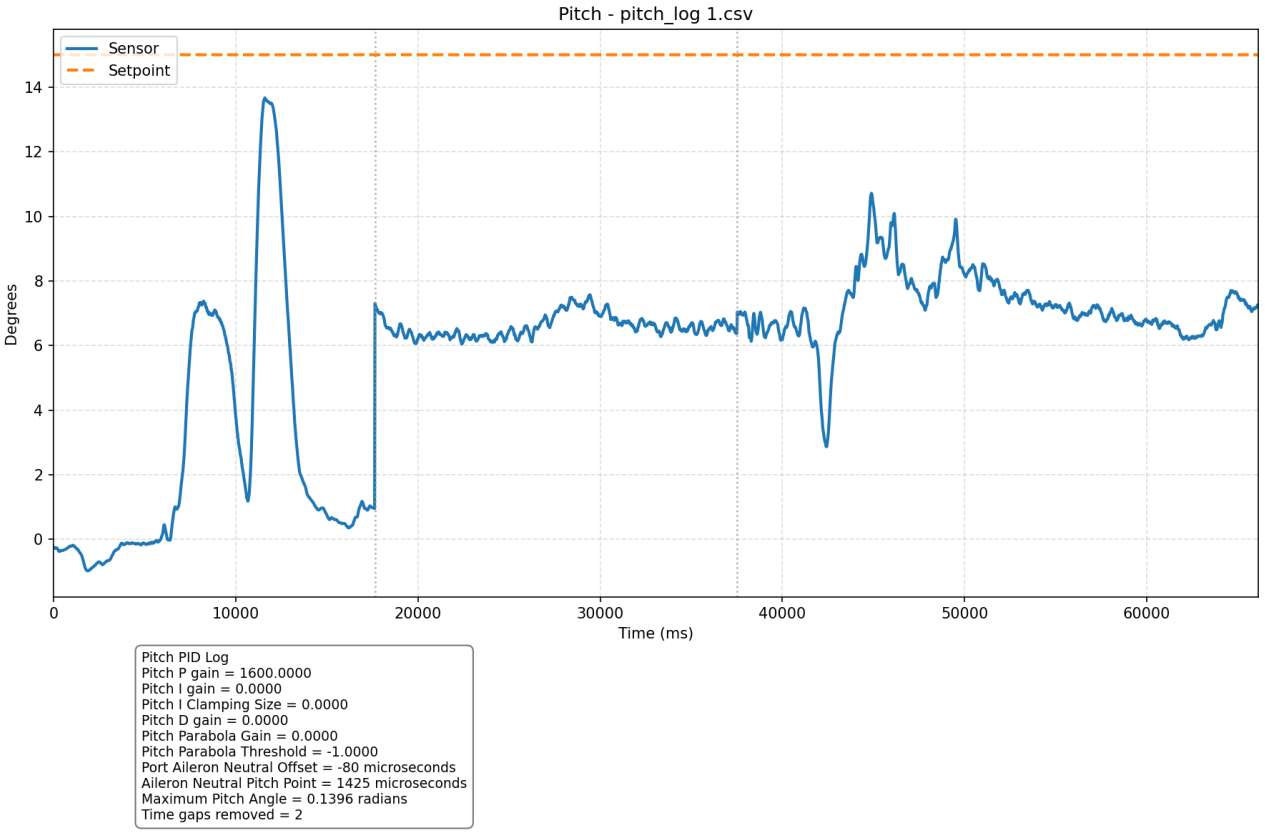

Figure 29 Test 1 Pitch Graph

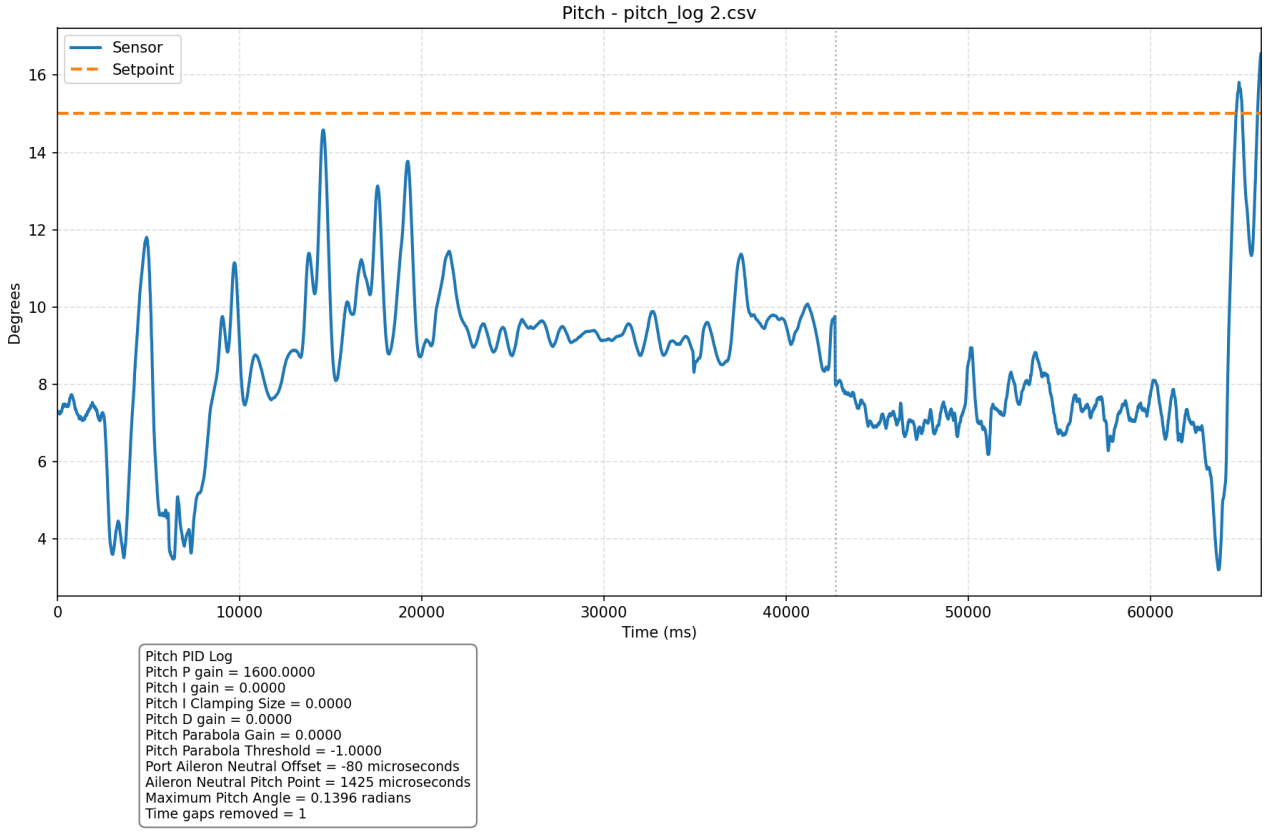

Figure 30 Test 2 Pitch Graph

The pitch response log shown in Figure 29 demonstrates the behaviour of the active foil system while attempting to maintain a pitch setpoint of 15 degrees throughout operation. During the initial acceleration and take-off phase, the pitch angle rapidly increased as the board attempted to transition onto foil. Several transient spikes were observed early in the run, with measured pitch angles approaching approximately 13–14 degrees before settling into a more stable operating region. These initial peaks likely correspond to rapid lift generation and rider input during foil take-off. Following this transition phase, the measured pitch angle stabilised and remained relatively consistent throughout much of the run. For a large portion of the test duration, the pitch angle operated between approximately 6 and 8 degrees, demonstrating that the board was capable of maintaining sustained foiling conditions despite the increased drag generated by the custom hydrofoil assembly. However, the measured pitch angle consistently remained below the desired 15-degree setpoint, indicating that the system was unable to generate sufficient lift to achieve the target operating attitude. Several transient pitch disturbances remained visible throughout the run, particularly during unstable foiling periods where rapid pitch fluctuations and spikes occurred before the system returned to a more stable operating region.

Similar behaviour was observed within the second pitch response test shown in Figure 30. During the early stages of the run, transient spikes again occurred with measured pitch angles approaching approximately 14–15 degrees before stabilising. The system then settled into a relatively stable operating region where the measured pitch angle generally fluctuated between approximately 7 and 10 degrees for much of the run. Although the pitch response demonstrated smaller oscillations than the roll response, several transient spikes and rapid fluctuations remained visible throughout testing, particularly near the end of the run where unstable foil behaviour occurred. The inability to consistently achieve the desired 15-degree pitch setpoint directly correlates with the increased hydrodynamic drag generated by the larger custom wing assembly. The increased drag reduced achievable board speed and therefore limited lift generation capability. Despite this limitation, the pitch controller remained responsive throughout testing and demonstrated the ability to maintain partial pitch stability during sustained hydrofoil operation.

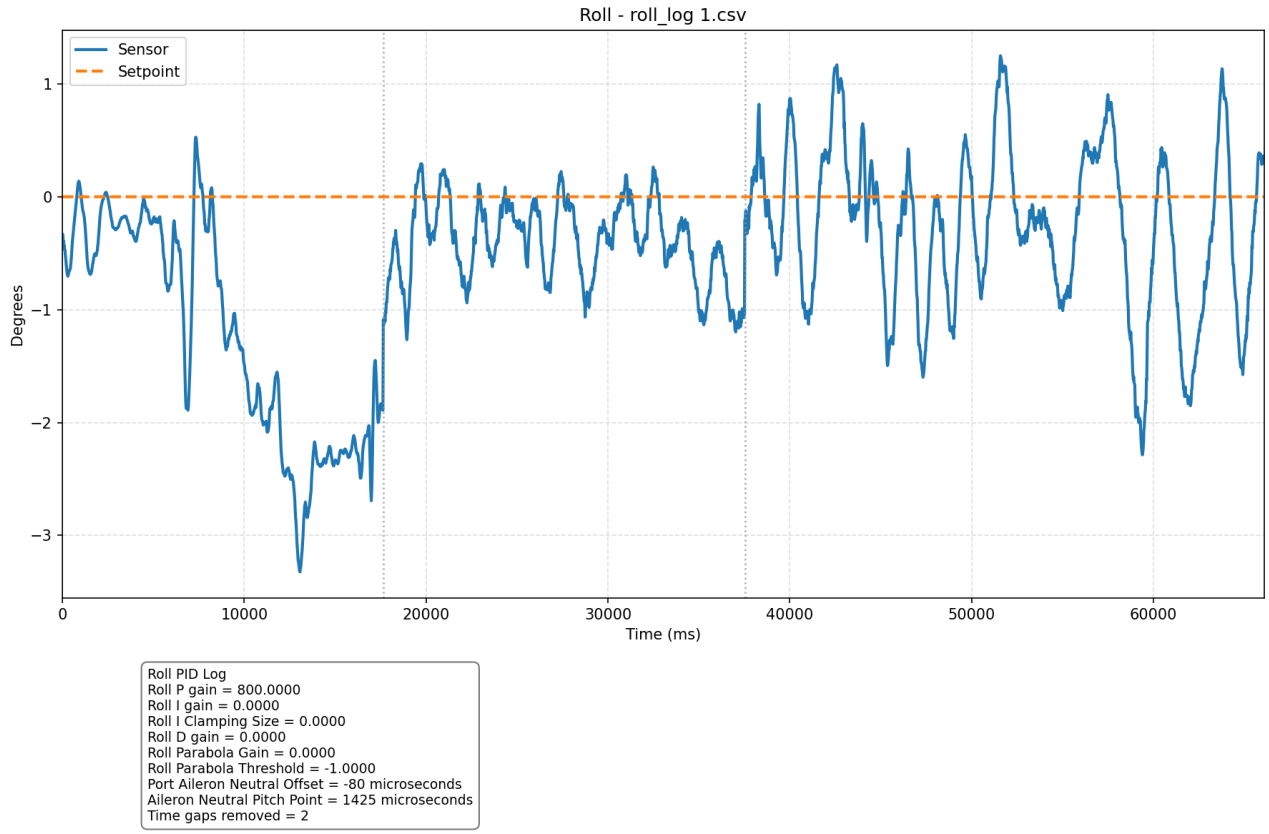

Figure 31 Test 1 Roll Graph

The selected roll response log shown in Figure 31 demonstrates that the active stabilisation system was capable of actively responding to roll disturbances during hydrofoil operation. Throughout testing, the roll controller attempted to maintain a target roll angle of 0 degrees. During the early stages of the run, the measured roll angle remained relatively stable, generally oscillating within approximately ±1 degree of the setpoint. This indicates that the active ailerons were successfully generating corrective roll moments and compensating for smaller disturbances encountered during lower-speed and early foiling conditions. As the run progressed, the magnitude of the oscillations gradually increased, with repeated oscillatory behaviour becoming visible around the setpoint. Despite this oscillation, the system generally remained within a controlled operating range of approximately -2 degrees to +1 degree for much of the run. Larger transient disturbances became visible near the end of the test, where roll deviations approached approximately -3.3 degrees. These

disturbances likely correspond to unstable foiling conditions, rider movement, or changing hydrodynamic loading during operation.

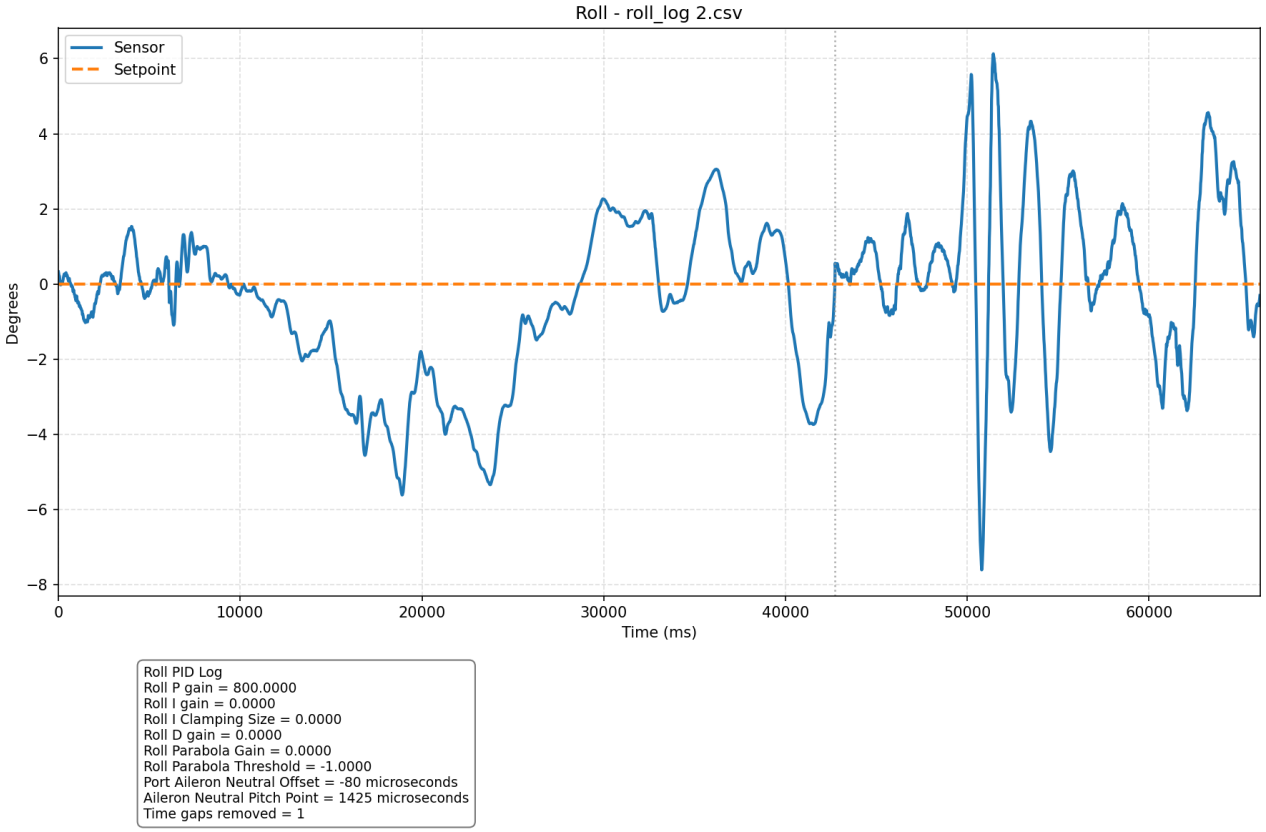

Figure 32 Test 2 Roll Graph

The second roll response test shown in Figure 32 exhibited significantly larger oscillations throughout operation. During later sections of the run, repeated alternating roll disturbances occurred around the setpoint, with peak values approaching approximately +6 degrees and -7.5 degrees. Compared to the first roll test, the second run demonstrated substantially more aggressive oscillatory behaviour and larger overshoot responses from the controller. This behaviour likely resulted from increased unstable foiling conditions, wave interaction, and rider-induced disturbances. The roll response also demonstrated that the proportional-only controller tuning used throughout testing was relatively aggressive for the dynamic behaviour of the hydrofoil system. With a proportional gain of 800 and both integral and derivative gains disabled, the controller responded rapidly to disturbances but lacked sufficient damping to prevent overshoot and continuous oscillatory correction behaviour. As hydrodynamic loading increased, the active ailerons generated increasingly large corrective forces, contributing to the unstable oscillations visible throughout the later sections of both roll tests.

Overall, the testing demonstrated that the active stabilisation system successfully achieved closed-loop control of both the roll and pitch axes during real-world hydrofoil operation. The onboard IMU, ultrasonic sensing system, waterproof servo mechanisms, and servo-actuated ailerons were capable of detecting orientation changes and actively generating corrective control inputs in response to disturbances. While the system successfully maintained partial stability during sustained foiling operation, the results demonstrated that further controller tuning and hydrodynamic optimisation would be required to improve overall stability and reduce oscillatory behaviour. Future improvements would likely include implementation of derivative control to improve damping behaviour, refinement of proportional gain tuning, and reduction of wing thickness and structural mass to decrease hydrodynamic drag and improve lift generation capability.

Challenges and Failures

Throughout the development and testing of the active hydrofoil system, several significant challenges and failures were encountered relating to waterproofing, manufacturing, structural integrity, and hydrodynamic performance.

One of the first major failures occurred during the initial on-water test, where water ingress into the electronics enclosure caused damage to the onboard IMU sensor as seen in Figure 33. The original waterproofing approach proved insufficient for the marine environment, particularly around cable entry points and enclosure interfaces. To resolve this issue, the enclosure seals were improved, and additional waterproofing measures were introduced. Sponges were placed inside the cable gland enclosure and between the secondary switch enclosure and main electronics enclosure to absorb any water entering the system. These modifications significantly improved waterproof reliability during later testing.

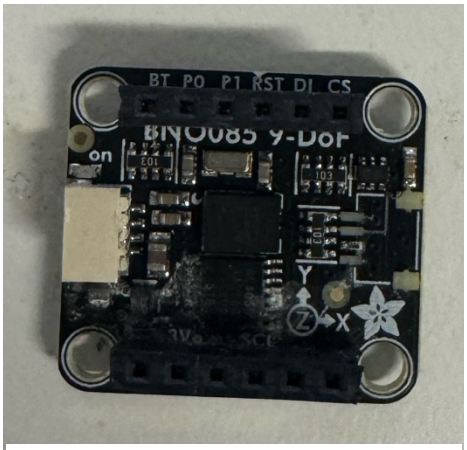

Figure 33 Water Damaged BNO085

Manufacturing the hydrofoil wing using large-format FDM 3D printing also presented several challenges. Due to the large size and length of the wing, prints were susceptible to instability and occasional failure during long print operations. Several tall prints experienced movement or collapsed during printing, requiring additional support structures and reprints. Dimensional accuracy was also an issue, with circular holes frequently printing as slightly oval shapes. This created fitment and alignment problems for the 6 mm pivot rod and aluminium extrusion, requiring additional post-processing and refinement before assembly.

The custom hydrofoil wing also significantly increased hydrodynamic drag compared to the original factory wing. The larger and thicker printed structure increased overall weight and resistance in the water, reducing the maximum board speed from approximately 24 km/h to 12 km/h. This made it difficult for the board to naturally rise onto foil, often requiring the rider to manually pump the board to assist lift generation.

A critical structural failure occurred approximately one hour into testing when the primary wing mounting section fractured, causing the front hydrofoil assembly to detach from the board as seen in Figure 34. This failure highlighted the high structural loads experienced during foiling operation and the limitations of the printed mounting structure. Safety ropes had been incorporated into the design prior to testing, successfully preventing the detached wing from being lost underwater and allowing safe recovery of the system.

Figure 34 Wing Mount Failure

Several improvements were identified for future development. Replacing critical structural components with composite or aluminium parts would significantly improve strength and durability. Reducing wing thickness and weight would help decrease drag and improve foiling efficiency. From a control perspective, implementing derivative control within the stabilisation system would improve damping and reduce oscillatory behaviour during operation. Additional waterproofing improvements, including marine-grade enclosures and improved sealing methods, would also improve long-term reliability in harsh marine environments.

Conclusion

This project successfully demonstrated the feasibility of implementing an actively stabilised electric hydrofoil system using low-cost embedded electronics, servo-actuated control surfaces, and large-format 3D printed components. The system successfully integrated waterproof electronics, onboard sensing, and closed-loop stabilisation control into a functional hydrofoil platform capable of real-world marine testing. The active stabilisation system demonstrated the ability to respond to roll and pitch disturbances during operation, validating the core concept of automatic foil control for e-foil applications.

Testing also highlighted several important limitations associated with the use of large-format FDM 3D printing for hydrofoil structures. The increased thickness and weight of the printed wing significantly increased hydrodynamic drag, reducing board speed and lift generation capability compared to the original factory hydrofoil. Structural and waterproofing failures encountered during testing further demonstrated the challenges associated with using printed thermoplastic components in high-load marine environments. These results provide valuable insight into the design considerations required when developing large 3D printed hydrofoil systems, particularly regarding structural reinforcement, waterproofing, print orientation, and hydrodynamic optimisation.

The project also serves as an important development platform for the REV Hydrofoil Jet Ski Generation 2 project. The e-foil board enabled rapid prototyping and validation of active stabilisation algorithms, waterproof electrical systems, and embedded control architectures before implementation on the larger hydrofoil jet ski platform. Lessons learned throughout the project, particularly regarding structural loading, controller tuning, and waterproof reliability, provide important guidance for future hydrofoil wing development and large-scale marine additive manufacturing within the Generation 2 system.

Overall, the project successfully validated the concept of active hydrofoil stabilisation while identifying several key areas for future improvement. The work completed establishes a strong foundation for continued development of actively controlled hydrofoil vehicles within the REV program and demonstrates the potential for low-cost rapid prototyping methods to support advanced marine research and development.

Bibliography

[1] G. Handl, “Decarbonising the Shipping Industry: A Status Report,” *The International Journal of Marine and Coastal Law,* vol. 38, no. 4, p. 730–791, 2023.

[2] The University of Western Australia, “The REV Project,” [Online]. Available: https://therevproject.com/vehicles/jetski.php.

[3] N. Perpitch, “Electric jet ski gives silent, surreal ride, its West Australian designers say,” ABC, 23 October 2015. [Online]. Available: https://www.abc.net.au/news/2015-10-23/uwa-students-design-electric-jet-ski/6880674.

[4] The Editorial Team, “Watch: Launch of world’s first electric hydrofoil jet ski,” SAFTEY4SEA, 9 August 2019. [Online]. Available: https://safety4sea.com/watch-launch-of-worlds-first-electric-hydrofoil-jet-ski/?utm_source=chatgpt.com.

[5] N. Cranenburgh, “This engineering startup is making waves with a flying electric watercraft,” Create Digital Engineers Australia, 27 August 2019. [Online]. Available: https://createdigital.org.au/engineering-startup-making-waves-flying-electric-watercraft/?utm_source=chatgpt.com.

[6] T. Wehrli, “Developing an Autonomous Hydrofoil with Waypoint Driving,” The University of Western Australua, 2024.

[7] T. Wehrli and T. Bräunl, “Autonomous Navigation and Automated Control for a Small Balancing Hydrofoil Craft,” *Journal of Marine Science and Engineering,* vol. 14, no. 1, pp. 0-50, 2026.

[8] E. D’Amato, I. Notaro, V. Piscopo and A. Scamardella, “Hydrodynamic Design of Fixed Hydrofoils for Planing Craft,” *Journal of Marine Science and Engineering,* vol. 11, no. 2, 2023.

[9] A. Eslamdoost, “Major climate benefits when ships “fly” over the surface,” Chalmers University of Technology, 2 June 2022. [Online]. Available: https://www.chalmers.se/en/current/news/m2-major-climate-benefits-when-ships-fly-over-the-surface/.

[10] J. Zhang, Z. Chang, Y. Zhang, G. Du, Z. Feng, Z. Yu, Y. Chu, B. Liang and H. Wang, “Dynamic analysis of hydrofoil flexibility in wave-powered boat propulsion performance,” *Ocean Engineering,* vol. 329, p. 121180, 2025.

[11] LILYGO, “T-Display S3,” 1 August 2022. [Online]. Available: https://lilygo.cc/products/t-display-s3?srsltid=AfmBOoqSWIC9d60UqL50Zgi6q1gnQbklYkGQtLo1BpRwaKYxMfHxPKM5. [Accessed 15 May 2026].

[12] AliExpress, “40KG HF3240SMG High Torque Digital Servo 180 Degree Metal Gear Brushless Motor Red for RC Car Robot Boat Industrial Use,” [Online]. Available: https://www.aliexpress.com/item/1005010311576324.html?src=google&src=google&albch=shopping&acnt=179-224-6891&isdl=y&slnk=&plac=&mtctp=&albbt=Google_7_shopping&aff_platform=google&aff_short_key=_oFgTQeV&gclsrc=aw.ds&albagn=888888&ds_e_adid=&ds_e_matchtype=. [Accessed 15 May 2026].

[13] Polulu, “Micro Maestro 6-Channel USB Servo Controller (Assembled),” [Online]. Available: https://www.pololu.com/product/1350. [Accessed 15 May 2026].

[14] DFROBOT, “A02YYUW Waterproof Ultrasonic Sensor for Arduino / ESP32 / Home Assistant (IP67, 3~450cm, UART),” [Online]. Available: https://www.dfrobot.com/product-

1935.html?srsltid=AfmBOooP-18p2uBc-tna8mV1C7Twe3Q-BdJQjyJOCCJrpq89C8ZfLKxJ. [Accessed 15 May 2026].

[15] AliExpress, “7.4V 1050mAh 2000mAh 3000mAh 11.1V 3S 2500 5200mAh Original And Upgrade Lipo Battery For MJX 16207,16208,14301,14210,10208,H8H,” [Online]. Available: https://www.aliexpress.com/item/1005005922732310.html?spm=a2g0o.order_list.order_list_main.261.78f81802tRiLmo. [Accessed 15 May 2026].

[16] AliExpress, “DC 30V to 5V Buck Converter Mini Voltage Regulator Board DC 6-30V Step Down to 5V 9V 12V 3A Power Supply Stabilizer Module,” [Online]. Available: https://www.aliexpress.com/item/1005006042537685.html?spm=a2g0o.order_list.order_list_main.185.78f81802tRiLmo. [Accessed 15 May 2026].

[17] A. Tools, “NACA 2412 Airfoil,” [Online]. Available: http://airfoiltools.com/airfoil/details?airfoil=naca2412-il.

[18] D. Akgumus, “Characterization of NACA 2412 and NACA 4412 airfoils: Effects of angle of attack on aerodynamics coefficients,” *Journal of Thermal Engineering,* p. 1524–1538, 2024.

[19] A. Pilots, “How the NACA 2412 Aerofoil Saves You Energy,” 31 May 2022. [Online]. Available: https://www.absolutepilots.com/en/how-the-naca-2412-aerofoil-saves-you-e/.

[20] Adafruit, “Adafruit 9-DOF Orientation IMU Fusion Breakout - BNO085 (BNO080) - STEMMA QT / Qwiic,” 2023 December 22. [Online]. Available: https://www.adafruit.com/product/4754?srsltid=AfmBOoow-0fChmsPH2PWd0lFPvZHcYleI1b2DKxS_C0ujpXHEM6XoR6H. [Accessed 15 May 2026].

[21] O. FDM, “1.75 mm PETG Basic Filament - 1 KG,” [Online]. Available: https://ozfdm.com.au/products/1-75-mm-petg-basic-filament-1-kg?variant=51282112872730&country=AU&currency=AUD&utm_medium=product_sync&utm_source=google&utm_content=sag_organic&utm_campaign=sag_organic&srsltid=AfmBOorAI1weT_Ah5kMBwjP_hACJJutc_dm50_c4vAnx1J. [Accessed 15 May 2026].

[22] Bunnings, “https://www.bunnings.com.au/metal-mate-19-x-19-x-1-2mm-1m-aluminium-square-tube-silver-1m_p1067807,” [Online]. Available: https://www.bunnings.com.au/metal-mate-19-x-19-x-1-2mm-1m-aluminium-square-tube-silver-1m_p1067807. [Accessed 15 May 2026].

[23] Ebay, “304 Stainless Steel Round Bar Solid Rod 6mm | Cut to Size 100–1000mm | DIY Craft,” [Online]. Available: https://www.ebay.com.au/itm/277429993082?chn=ps&_ul=AU&norover=1&mkevt=1&mkrid=705-139619-5960-0&mkcid=2&mkscid=101&itemid=277429993082&targetid=2449241580948&device=c&mktype=pla&googleloc=9191070&poi=&campaignid=23647363865&mkgroupid=196896323169&rlsatar. [Accessed 15 May 2026].

Appendix

Appendix 1 Web Server (see next page)

HYDROFOIL CONFIG

↓ Roll CSV | ↓ Pitch CSV | ↓ Altitude CSV

PID LOG STATUS		
Roll	0 / 12000	Reset
Pitch	0 / 12000	Reset
Altitude	0 / 2400	Reset

PARAMETER	VALUE	
Roll P gain	800.0000	Set
Roll I gain	0.0000	Set
Roll I Clamping Size	0.0000	Set
Roll D gain	0.0000	Set
Roll Parabola Gain	0.0000	Set
Roll Parabola Threshold	−1.0000	Set
Pitch P gain	800.0000	Set
Pitch I gain	0.0000	Set
Pitch I Clamping Size	0.0000	Set
Pitch D gain	0.0000	Set
Pitch Parabola Gain	0.0000	Set
Pitch Parabola Threshold	−1.0000	Set
Altitude P gain	0.0005	Set
Altitude I gain	0.0000	Set
Altitude I Clamping Size	0.0000	Set
Altitude D gain	0.0000	Set
Altitude Parabola Gain	0.0000	Set
Altitude Parabola Threshold	−1.0000	Set
Port Aileron Neutral Offset microseconds	−80	Set
Aileron Neutral Pitch Point microseconds	1425	Set
Cruising Height millimetres	350.0000	Set
Maximum Pitch Angle radians	0.1396	Set
Port Servo ID	0	Set
Starboard Servo ID	5	Set